T_n denotes the Chebyshev function of the first kind of order n

S_{12}^2 = power transferred from port 1 to 2
S_{14}^2 = power transferred from port 1 to 4

where

$$\frac{1}{\cos\theta_0} = \cosh\left(\frac{1}{n}\cosh^{-1}\beta/h\right) \tag{17}$$

and the pass band extends from θ_0 to $\pi-\theta_0$. Another relationship for the constants β and h can be obtained by applying the condition that the coupling ripple, in db, is to be symmetrical about the nominal coupling value. This condition gives

$$10\log_{10}\left[\frac{\beta^2-h^2}{1+\beta^2-h^2}\times\frac{\beta^2}{1+\beta^2}\right] = 2C \tag{18}$$

where C is the nominal coupling value in db.

The results of this synthesis for a two-section asymmetric coupler will be repeated here.

$$Z_{oe_1} = \frac{b}{d+1} \qquad Z_{oe_2} = dZ_{oe_1}. \tag{19}$$

Z_{oe_1} and Z_{oe_2} are the normalized even-mode impedances of the two-section coupler shown in Fig. 1(b). For a coupler with a specified coupling value and bandwidth, the values of β and h can be determined from (17) and (18). The constants b and d are defined in terms of β and h as follows:

$$b = \sqrt{(1+\beta^2)+(\beta+h)\sqrt{1+\beta^2}+\beta h} + \sqrt{(1+\beta^2)-(\beta+h)\sqrt{1+\beta^2}+\beta h} + \sqrt{2\beta(\beta+h)} \tag{20}$$

$$d = \sqrt{1+\beta^2-h^2}-\sqrt{\beta^2-h^2}. \tag{21}$$

The normalized odd-mode impedances can be obtained from the relationship

$$Z_{oe_1}Z_{oo_1} = Z_{oe_2}Z_{oo_2} = 1. \tag{22}$$

It has been shown by several investigators that (22) represents the condition for which, independent of frequency, the coupler is matched and has infinite directivity.[9,10]

ACKNOWLEDGMENT

The author wishes to thank L. Teichman for his significant help in performing the measurements.

[9] E. M. T. Jones and J. T. Belljahn, "Coupled-strip-transmission-line filters and directional couplers," IRE TRANS. ON MICROWAVE THEORY AND TECHNIQUES, vol. MTT-4, pp. 75–81; April, 1956.
[10] J. K. Shimzer and E. M. T. Jones, ""Coupled-transmission-line directional couplers," IRE TRANS. ON MICROWAVE THEORY AND TECHNIQUES, vol. MTT-6, pp. 403–410; October, 1958.

Synthesis of Filter-Limiters Using Ferrimagnetic Resonators

R. L. COMSTOCK, MEMBER, IEEE

Summary—A synthesis procedure is developed for microwave band-pass filters with the Chebyshev response using orthogonal circuit resonators coupled by a ferrimagnetic resonator. A stripline ferrimagnetic resonator filter is analyzed in detail. Equations and graphs are given which allow the selection of ferrimagnetic material and size of the ferrimagnetic sample necessary to achieve a desired bandwidth and insertion loss for a given pass-band response. The theoretical behavior of these circuits as microwave power limiters is discussed and it is shown that the ratio of the limiting threshold to the filter bandwidth is a constant depending only on the pass band response shape. Experimental confirmation of the design information is discussed as well as some practical methods of varying the limiting threshold.

Manuscript received June 6, 1964; revised July 24, 1964.
The author is with the Lockheed Missiles and Space Company, Research Laboratories, Palo Alto, Calif. He was formerly with the Bell Telephone Laboratories, Inc., Murray Hill, N. J.

I. INTRODUCTION

THE COUPLING of small ferrimagnetic ellipsoids to microwave transmission lines has been discussed by a number of authors [1]–[3]. It is found that when the ferrimagnet is excited in the uniform precession it behaves like a lumped constant resonator with, in certain cases, a nonreciprocal phase behavior. The resonant frequencies of such a resonator can be tuned with a dc magnetic field. Its unloaded $Q(Q_u)$ depends on the surface polish of the sample and doping with impurity ions. For example, with highly polished yttrium iron garnet (YIG) spheres Q_u can be as great as 10,000 at C band. It is further observed that the coupling to such a resonator can be tight enough to allow a

large amount of energy transfer through the resonator, and with the large unloaded Q's available, with low insertion loss. This paper will extend these results by discussing the coupling of ferrimagnetic resonators not to transmission lines but rather to a class of resonant microwave circuits. It is shown that ferrimagnetic resonators can be fitted into the scheme developed by Dishal [4] and Taub and Bogner [5] for optimizing direct coupled resonator filters using lumped elements. Also, the use of ferrimagnetic filter structures as microwave power limiters will be discussed; in particular, a detailed analysis of the resonant stripline circuit first described by De Grasse [1] will be presented.

In order to use the results given by Dishal, and Taub and Bogner, it is necessary to describe the microwave resonators by lumped-constant equivalent circuits. This always can be done providing the results are not extended to large (>10 per cent) bandwidths. The lumped-element equivalent circuit of the ferrimagnetic resonator is also only valid over a small bandwidth since, in general, the element values are functions of frequency. In case it is desired to develop devices having even larger bandwidths, the design procedure developed by Cohn [6] for wideband direct-coupled resonator filters can be extended to include ferrimagnetic resonators in a similar manner.

II. The Ferrimagnetic Resonator and Dipolar Coupling

In this section some properties of the ferrimagnetic resonator along with some information on microwave circuit coupling to be used in the next section on band-pass filter synthesis will be discussed.

The important parameters for describing a resonator are its unloaded $Q(Q_u)$ and degree of coupling. For a generalized ellipsoidal ferrimagnetic sample excited in the uniform precession magnetostatic mode the unloaded Q is,

$$Q_u = \frac{\omega_0}{2\eta_0}, \tag{1}$$

where η_0 is a loss parameter which in the case of a sphere is given by $\mu_0\gamma\Delta H/2$ where ΔH is the resonance linewidth, and ω_0 is the uniform precession resonance frequency $=\mu_0\gamma H_0$ for spheres, where H_0 is the external dc magnetic field.

In general there are other microwave resonances that can exist in these samples, *e.g.*, magnetostatic modes and short wavelength spin waves. While magnetostatic modes (other than the uniform precession) may be important in certain applications of ferrimagnetic resonators, they will not be discussed further in the theoretical part of this paper since they have not proven to be of significance in the experiments to be described (Section VI). The effects of spin waves on the properties of these resonators will be discussed in the section on limiting.

It is desired to extend the theory of lumped-element band-pass transmission type filters consisting of direct-coupled resonators to include ferrimagnetic resonators. It is necessary to have input and output ports for each resonator which are uncoupled except by energy transfer through the resonator. As shown by De Grasse [1], this can be achieved by coupling normally orthogonal microwave circuits through transverse components of the dipolar fields of a ferrimagnetic sphere excited in the uniform precession mode [*e.g.*, see Fig. 1(a)]. These orthogonal circuits can be crossed wires, loops, striplines, waveguides, cavity modes, etc.

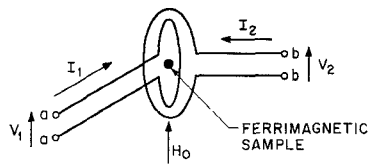

(a)

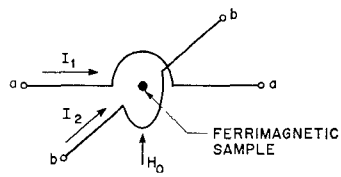

(b)

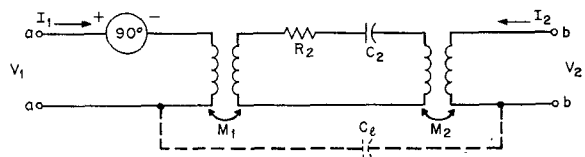

$$V_1 = \frac{j\omega^3 M_1^2/L_2}{\omega_0^2-\omega^2+j\omega\omega_0/Q_0} I_1 + \frac{j\omega^3 M_1M_2/L_2}{\omega_0^2-\omega^2+j\omega\omega_0/Q_0} I_2$$

$$V_2 = -\frac{j\omega^3 M_1M_2/L_2}{\omega_0^2-\omega^2+j\omega\omega_0/Q_0} I_1 + \frac{j\omega^3 M_2^2/L_2}{\omega_0^2-\omega^2+j\omega\omega_0/Q_0} I_2$$

(c)

Fig. 1—Loop (a) and semi-loop coupling (b) by a ferrimagnetic sphere. The equivalent circuit representation (c) for these circuits derived from (10) and (11) also is shown along with the circuit equations.

The dipolar coupling between a ferrimagnetic sample and a pair of orthogonal circuits can be calculated by assuming currents to exist in the two circuits which create magnetic fields at the position of the dipole. A vector operator can then be defined,

$$I = \begin{pmatrix} I_1 \\ I_2 \end{pmatrix}, \tag{2}$$

where I_1 and I_2 are the currents in the two orthogonal circuits. The resulting external magnetic field at the sample is then,

$$h^e = \begin{pmatrix} h_x \\ h_y \end{pmatrix} = C \cdot I, \tag{3}$$

where,

$$C = \begin{pmatrix} C_{12} & 0 \\ 0 & C_{23} \end{pmatrix} \tag{4}$$

is a coupling matrix whose elements depend only on the geometry of the circuit and the position of the sample [2]. The rectangular coordinates x, y are centered at the center of symmetry of the sample. The transverse magnetization in the sample is

$$\boldsymbol{m} = \chi^e \cdot \boldsymbol{h}^e = \chi^e \mathbf{C} \cdot \boldsymbol{I}, \tag{5}$$

where χ^e is the external susceptibility tensor for the ferrimagnetic sample, the components of which are, in the case of a sphere,

$$\chi_{xx}{}^e = \chi_{yy}{}^e = \frac{\omega_M \omega_0}{\omega_0^2 - \omega^2 + 2j\eta_0\omega_0} \qquad \chi_{xy}{}^e = \chi_{yx}{}^e = \frac{\omega_M \omega}{\omega_0^2 - \omega^2 + 2j\eta_0\omega_0}, \tag{6}$$

where $\omega_M = \gamma\mu_0 M$. The voltages induced in the two orthogonal circuits are given by

$$V_i = j\omega \int_{\text{circuit } i} \boldsymbol{b} \cdot d\boldsymbol{a}, \qquad i = (1, 2), \tag{7}$$

where $\boldsymbol{b}$ is the magnetic induction arising from the magnetic dipolar fields and $V_{1,2}$ is identified with the $i=1$ and $i=2$ integrals, respectively. The maximum dipolar induction is given by

$$\boldsymbol{b} = \mu_0 \boldsymbol{h} = \mu_0 \frac{\boldsymbol{m} v_s}{2\pi r^3}, \tag{8}$$

where r is the radial distance from the magnetic dipole and $v_s = (\pi/6)(D_s)^3$ is the volume of the sample. After combining the above equations it is found that

$$V_i = \frac{j\omega\mu_0 v_s}{2\pi} \int_{\text{circuit } i} \frac{\chi^e \cdot \mathbf{C} \cdot \boldsymbol{I} \cdot d\boldsymbol{a}}{r^3}. \tag{9}$$

As an example of the use of this result consider the coupling to two identical orthogonal loops (radius r_0) by a spherical sample in the geometrical center as shown in Fig. 1(a). In this case

$$\boldsymbol{h}^e = \frac{1}{2r_0} \boldsymbol{I}$$

and

$$C_{12} = C_{23} = \frac{1}{2r_0}.$$

When integrated over the area of the loops, (3) results in

$$\boldsymbol{V}_{\text{loop}} = \begin{bmatrix} V_1 \\ V_2 \end{bmatrix}_{\text{loop}} = j\omega\mu_0 \frac{v_s}{2r_0^2} \begin{bmatrix} \chi_{xx}{}^e I_1 + \chi_{xy}{}^e I_2 \\ \chi_{yx}{}^e I_1 + \chi_{yy}{}^e I_2 \end{bmatrix}, \tag{10}$$

where in this case I_1 and I_2 are currents flowing in the loops and V_1 and V_2 are voltages developed around the loops. Eq. (9) has been previously derived by De Grasse [1] and Carter [2]. In the remainder of this paper the analysis will be restricted to the coupling between ferrimagnetic spheres and "necked-down" striplines whose shapes in the vicinity of the sample are in the form of semi-loops as shown in Fig. 1(v). For this case the coupling is approximately half that for the full loop, resulting in

$$\boldsymbol{V}_{\frac{1}{2}\text{ loop}} = \begin{bmatrix} V_1 \\ V_2 \end{bmatrix}_{\frac{1}{2}\text{ loop}} = \frac{j\omega\mu_0 v_s}{8r_0^2} \chi^e \cdot \boldsymbol{I}. \tag{11}$$

An equivalent lumped electrical circuit can be found to represent (11), and using (6) the result is shown in Fig. 1(c). The circuit equations given in the figure are of the same form as (10) and (11). The nonreciprocal phase characteristic of the gyromagnetic coupler is indicated by the fact that $\chi_{xy}{}^e = -\chi_{yx}{}^e$ and is shown in the equivalent circuit by the nonreciprocal 90° phase shift. The nonreciprocal phase shift is demonstrated experimentally in Section VI.

The ferrimagnetic sample appears as a resonator inductively coupled to the wire semi-loops. The lumped constant equivalent circuit for the semi-loop coupled ferrimagnetic resonator can now be used in any of the available synthesis procedures for band-pass filters. As an example, the synthesis procedure developed by Dishal [4] and extended by Taub and Bogner [5] will be generalized to include these resonators. Dishal's synthesis procedure provides values of the coupling coefficients and loaded Q's of lumped constant direct coupled resonators which are necessary to achieve a specified pass-band response. In the case of inductively coupled resonators the coupling coefficients provided by Dishal's procedure are

$$K_{12,23} = \frac{M_{1,2}}{\sqrt{L_{1,3}L_2}},$$

where $L_{1,3}$ is the series inductance connected across terminals aa and bb of the circuit in Fig. 1(c), respectively. By comparing the original parameters for the ferrimagnetic resonator from (11) and the equivalent circuit parameters from Fig. 1(c), the coupling coefficient for a semiloop results,

$$K^2{}_{12,23} = \frac{\mu_0 v_s}{L_{1,3}} \frac{\omega_M}{\omega_0} \frac{1}{8r_0^2}. \tag{12}$$

The inductances L_1 and L_3 are the inductances of the series LC equivalent circuits for the microwave resonators coupled to the ferrimagnetic resonator. The inductances are calculated for TEM resonators in Section IV by making the resonant frequencies and reactance slopes equal for the actual and lumped equivalent circuits. In the following analysis only symmetrical networks will be considered for which $K_{12} = K_{23} = K$.

III. Band-Pass Filter Synthesis

Dishal has analyzed a class of lumped-constant band-pass circuits which have specified pass-band characteristics as shown in Fig. 2. This response shape is the well-known Chebyshev response which reduces to the maximally flat response in the limit of vanishing pass-band ripple amplitude.[1] Dishal's analysis allows the specification of response shape for a filter but does not allow for a specification of the minimum insertion loss ($l_{\min}$). Taub and Bogner have analyzed *three* resonator band-pass filters of the type considered by Dishal and using his equations have imposed the additional constraint of minimum insertion loss in the pass band. Their results will be used in what follows and the analysis is restricted to three resonator structures.

The circuits considered by Dishal consist of shunt (series) resonators coupled by series (shunt) lumped elements. Schematically the three resonator filter appears as shown in Fig. 3. The results of the synthesis procedure developed in [4] and [5] for band-pass filters are indicated briefly in this section with the circuit parameters defined as follows:

$d = 1/Q$ = total resonant circuit decrement.
$\delta = d/(\Delta f/f_0)$ = normalized decrement.
$\Delta f/f_0$ = total 3-db fractional bandwidth.
f_0 = resonant frequency of each resonant circuit.
$\omega_0 = 2\pi f_0$ = angular resonant frequency.
K_{ij} = resultant coefficient of coupling between resonant circuits.
$k_{ij} = K_{ij}/\Delta f/f_0$ = normalized coefficient of coupling $= K_{ij}Q_L$.
l = midband insertion loss in db.
P_a = available input power.
P_{out} = output power.
$Q_1 = Q$ of first resonant circuit loaded only by the input.
$Q_2 = Q_u$ = unloaded Q of resonators (assumed equal).
$Q_3 = Q$ of third resonant circuit loaded only by the output.
$Q_L = f_0/\Delta f$.

Dishal has shown that for a specified over-all bandwidth the required minimum unloaded Q (or maximum value of δ_2, $\delta_{2\max}$) for the resonators (assumed to be the same[2]) is specified completely by the ripple level (peak to valley ratio of the transmission coefficient) in the pass band; for example, with 0 db and 0.5 db pass-band ripple the value of $\delta_{2\max} = Q_L/Q_{0\min}$ is 0.5 and 0.271 respectively [5]. Taub and Bogner have shown that the minimum insertion loss in the pass band which, along with the ripple level, describes the pass band can be specified approximately for any ripple level by a specification of $\delta_2/\delta_{2\max}$. For $l_{\min} < 2$ db, their results show

$$l_{\min} \approx 10 \frac{\delta_2}{\delta_{2\max}} = \frac{10 f_0}{\Delta f Q_u \delta_{2\max}}, \tag{13}$$

where $l_{\min}$ is expressed in db. In the limit of vanishing insertion loss the coupling coefficient $k_{12} = k_{23} = k$ and $\delta_1 = \delta_3$ depend only on the pass-band ripple; for example, with 0 db and 0.5 db pass-band ripple the normalized coupling coefficients are $k = 0.7$ and 0.65 and the normalized resonator decrements are $\delta_1 = 1.0$ and 0.55, respectively. Extensive curves of k and δ_1 for various values of $\delta_{2\max}$ vs $\delta_2/\delta_{2\max}$ and hence ripple level are given in [5].

No consideration has been given so far to the shape of the filter characteristic outside the pass band. For an n resonator filter the skirt selectivity (sharpness of the filter cutoff) increases rapidly as n increases.[3] In case the selectivity resulting from a 3 resonator (3 pole) filter is inadequate for the requirements at hand it will be necessary to extend these results for $n > 3$.

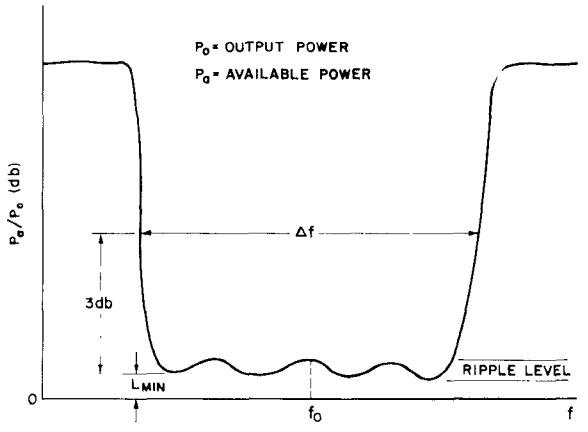

Fig. 2—Specification of band-pass filter characteristic.

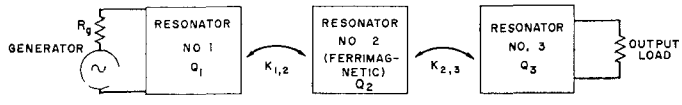

Fig. 3—Block diagram of three resonator filter.

IV. Crossed Stripline Filter

The information given in Section II on ferrimagnetic resonators and in Section III on band-pass filters will now be combined to show how a 3-resonator filter using a ferrimagnetic resonator as the center resonator can be synthesized. First, a choice must be made as to what type of resonator will be used as the first and last resonator. The resonators which will be discussed here are resonant sections of strip transmission line with a semi-loop located in the center (Fig. 4) as first described by

[1] These pass-band responses are optimum in the sense of having the sharpest cutoff in the stop band for a given pass-band ripple.

[2] As shown in [4] this is not a serious limitation if all resonators exceed the minimum Q_u specified in [4].

[3] See, for example, "Reference Data for Radio Engineers," 4th Ed., International Telephone and Telegraph Corp.; 1956.

De Grasse [1]. The resonators can have $l_r/2 = n(\lambda/2)$ $(n = 1, 2, \cdots)$ in which case the ternimals must all be short circuited and coupling to external transmission lines supplied by, say, loops placed in the vicinity of the short circuits. It is also possible for $l_r/2 = n(\lambda/4)$ (n odd) in which case the terminals would need to be open circuited and coupling supplied by, say, series capacitance or quarter wavelength transmission lines. Note that coupling to external transmission lines is only necessary at the terminals marked "1" and "2," as shown in Fig. 4. The lumped constant equivalent circuit for one stripline resonator coupled to a ferrimagnetic resonator (located in the semi-loop as shown in Fig. 4) is shown in Fig. 5. The end couplings have been represented by coupled coils with mutual inductance $M_{0,3}$.[4] This representation of the end couplings can be shown to be quite general and will be used exclusively in what follows. The lumped element equivalent circuit for the stripline resonator can be found in a number of ways [7], one of which is to equate the slopes of the two reactance functions at resonance, *i.e.*,

$$\left.\frac{dX(\omega_0)}{d\omega}\right|_{\text{equivalent lumped constant resonator}} = \left.\frac{dX(\omega_0)}{d\omega}\right|_{\text{stripline resonator}}.$$

In case $l_r/2 = n(\lambda/2)$ (short circuit ends) this condition results in [7]

$$L_1 = Z_{01}\frac{n\pi}{\omega_0}$$

$$\omega_0^2 = \frac{1}{L_1C_1},$$

where Z_{01} is the characteristic impedance of the stripline resonators. If $l_r/2 = n\lambda/4$ (n odd for open circuit ends) the lumped elements are [7]

$$L_1 = \frac{Z_{01}n\pi}{4\omega_0}$$

$$\omega_0^2 = \frac{1}{L_1C_1}.$$

In arriving at the lumped constant equivalent circuit the resonator losses have been neglected. The losses will be represented by the unloaded resonator Q's. The results of Section II and the lumped element equivalent for the stripline resonators can be used to evaluate the coupling coefficient, $K = K_{1,2} = K_{2,3}$

[4] The coupling parameters $M_{0,3}$, can be calculated for a given microwave structure as shown in vol. 8 of the radiation Laboratory Series (Principles of Microwave Circuits). It has not been found necessary to carry out such a calculation since the end couplings are invariably adjusted experimentally. One convenient way to adjust the external Q's ($Q_{1,3}$) experimentally is to observe the signal reflected from the filter when the dc magnetic field for the ferrimagnetic resonator is adjusted far from resonance.

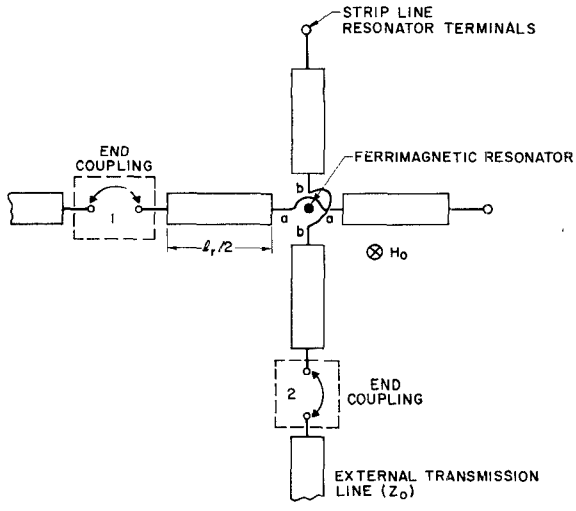

Fig. 4—Crossed strip-line filter with ferrimagnetic resonator.

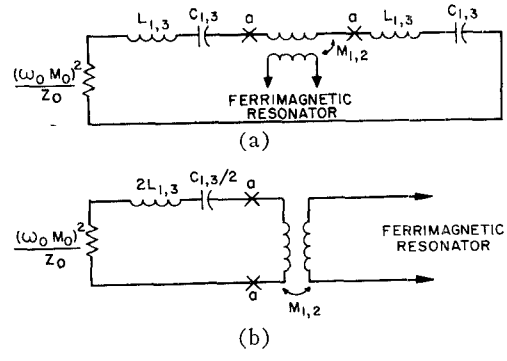

Fig. 5—Lumped equivalent circuit of strip-line resonator coupled to ferrimagnetic resonator.

$$K^2\Big|_{\text{short circuit ends}} = \frac{\mu_0 v_s \omega_M}{Z_{01}} \frac{1}{n\pi 8r_0^2} \left(\frac{l_r}{2} = \frac{n\lambda}{2}\right) \quad (14a)$$

$$K^2\Big|_{\text{open circuit ends}} = \frac{\mu_0 v_s \omega_M}{Z_{01}} \frac{1}{n\pi 2r_0^2} \left(\frac{l_r}{2} = n\frac{\lambda}{4},\ n \text{ odd}\right). \quad (14b)$$

The complete equivalent circuit for the crossed stripline ferrimagnetically coupled filter is shown in Fig. 6.

The experiments to be described in Section IV have been restricted to open circuit resonators and the design procedure will also be restricted to this case. Using the value for K given in (8) it is now possible to combine the results of this section with those of Section III resulting in a design procedure for these filters as follows:

1) Choose bandwidth, ripple level and maximum pass-band insertion loss.
2) From curves of $\delta_{2\max}$ vs pass-band ripple given in [5] and (7), evaluate the required minimum value for Q_u.
3) Evaluate the coupling coefficient and loaded resonator decrements from curves in [5].

4) From (8), evaluate the ratio $(\omega_m/Z_0)D_S^3/r_0^2$. These parameters can then be used in a trade-off in any convenient way.

To illustrate the above design considerations the following case is considered

$l_{max} = 0.5$ db
ripple $= 0.5$ db
$Z_{01} = 100\ \Omega$
$r_0 = 0.150''$
$4\pi M = 1750$, 3640 gauss.

The first value of $4\pi M$ is appropriate to yttrium iron garnet, and the second to lithium ferrite. From [5] (see Section III), the value of k is 0.65, and from (7), the minimum value for Q_u is found to be $7.38/(\Delta f/f_0)$. Using the normalized value of k given along with (8) it is possible to solve for the value of the required sphere diameter as a function of the 3-db bandwidth. The results of this calculation are shown in Fig. 7 for the two values of $4\omega M$. It is seen from the value of Q_u given above that extremely narrow lindwidths are not needed for low insertion loss filters with moderate bandwidths; for example, for 10 per cent bandwidth at S-band (3 Gc), $Q_u > 74$ or $\Delta H < 14.5$ oe. The loaded resonator Q's are then adjusted by adjusting the external coupling.

From the equivalent circuit given in Fig. 6, it is possible to relate the coupling coefficient to the easily measured mormal mode resonances of the three element filter under conditions that the input and the output of the filter are loosely coupled ($Q_1 \gg 1$). That is, K can be related to the frequencies ($\omega^{\pm}$) for which the input impedance vanishes when the output is open circuited. In the lossless case, this condition results in

$$(\omega^{\pm})^2 = \omega_0^2(1 \pm \sqrt{2}\,K), \quad \text{or}$$
$$K = \frac{(\omega^{+})^2 - (\omega^{-})^2}{2\sqrt{2}\,\omega_0^2}. \tag{15}$$

In Section VI measurements will be described of $\omega^{\pm}$ for various sphere diameters using yttrium iron garnet in a representative crossed stripline filter. These measurements can then be used to determine experimentally the coupling constant.

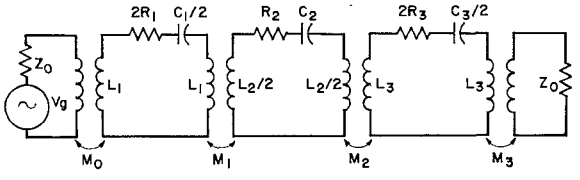

Fig. 6—Lumped constant equivalent circuit for strip-line ferrimagnetic resonator filter.

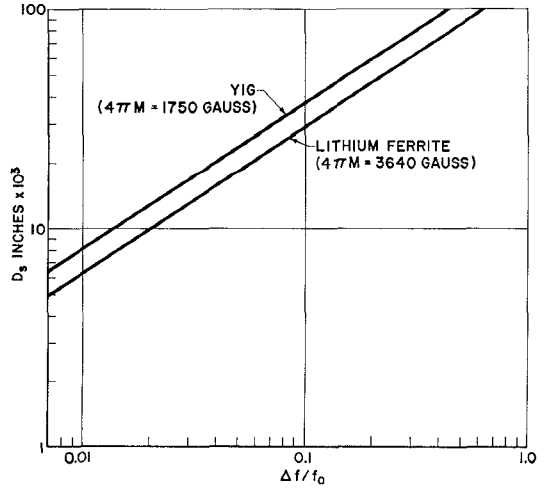

Fig. 7—Required diameter of YIG or lithium ferrite sphere for specified filter bandwidth for 0.5-db pass-band ripple.

V. Limiting

As has been discussed by Shul [8] the resonance susceptibility of a ferrimagnet can be expected to decrease above some critical value of transverse magnetization due to the parametric excitation of spin waves. In what follows only the first order spin wave instability [8] will be considered since it has resulted [9]–[12] in limiting characteristics which are superior to second order process limiters [13].

In the first order process, the resonance susceptibility has a constant value χ_0'' for RF fields less than a critical value, h_{crit} but declines as

$$\chi'' = \frac{\chi_0''}{h/h_{crit}} \tag{16}$$

for $h > h_{crit}$. The threshold field depends on the uniform precession and spin wave linewidths as discussed in [8].

The decline in the susceptibility leads to power limiting in filters of the type under consideration. This can be seen by rewriting (4) in terms of RF fields, with the assumption that all susceptibility components decline with magnetic field as given by (16),

$$V_1 = (V_1)_{crit} = \frac{j\omega\mu_0 v_s}{2\pi} \int_{\text{circuit 1}} [(\chi_{xx0}'')^e (h_x)_{crit} + (\chi_{xy0}'')^e (h_y)_{crit}] \frac{da}{r^3}$$
$$V_2 = (V_2)_{crit} = \frac{j\omega\mu_0 v_s}{2\pi} \int_{\text{circuit 2}} [(\chi_{yx0}'')^e (h_x)_{crit} + (\chi_{yy0}'')^e (h_y)_{crit}] \frac{da}{r^3}. \tag{17}$$

The voltages are limited since they are constants and no longer depend on the circuit currents.

The threshold output power for a limiter can be calculated once h_{crit} is known and such a calculation for the crossed stripline circuit described in Section IV is given below.

From Fig. 6 the impedance coupled into the output resonator is

$$Z_L = \frac{(\omega_0 M_3)^2}{Z_0},$$

and if the internal damping of the resonator is neglected, which is a satisfactory approximation for wide-band operation, the loaded resonator Q is

$$Q_3 = \frac{\pi Z_{03} Z_0}{4(\omega_0 M_3)^2}.$$

The output power from the limiter at the threshold is, again neglecting internal resonator losses,

$$(P_0)_{\text{crit}} = \frac{I^2_{\text{crit}}}{2} \frac{(\omega_0 M_3)^2}{Z_0},$$

and with

$$h_{\text{crit}} = I_{\text{crit}}/4r_0,$$

$$(P_0)_{\text{crit}} = \frac{h^2_{\text{crit}} Z_{03} 4r_0^2 \pi}{Q_3}.$$

The loaded resonators Q can be related to the over-all bandwidth of the filter by

$$\delta_3 = \frac{f_0/\Delta f}{Q_3},$$

which δ_3 is determined from information on the insertion loss and ripple level (see [5]). Thus

$$(P_0)_{\text{crit}} f_0/\Delta f = h^2_{\text{crit}} Z_{03} 4r_0^2 \pi \delta_3. \quad (18)$$

From this expression it is seen that for a given h_{crit}, fixed circuit geometry (r_0, Z_{01}), pass-band ripple, and insertion loss the ratio of threshold power to fractional bandwith is a constant. This result is reminiscent of the familiar (gain)$\times$(bandwidth) limitation of amplifiers and indicates that an increase in the bandwidth of the filter (*e.g.*, by using a larger sample) will raise the threshold of the limiter. Limiting thresholds as low as -35 dbm have been observed in narrow-band limiters using narrow linewidth single crystal yttrium iron garnet [9] while wide-band limiters ($\Delta f/f_0 > 10$ per cent) have been made which have thresholds in the milliwatt range as described in Section VI. The "dynamic range"[5] of these limiters is typically 25–30 db and is prevented from obtaining larger values by leakage represented in Fig. 1 by the capacitor C_l. The leakage capacitance can be minimized by making the mutual area of the crossed strip lines as small as possible commensurate with maintaining the minimum value of the unloaded resonator Q's. Capacitive shields between the strip lines have been used also.

VI. Experimental Results

First of all it is necessary to establish the validity of the equation for dipolar coupling given in Section IV. As mentioned in that section, it is possible to relate the coupling constant K to the normal mode resonances of the three-element filter. This relationship was checked experimentally by measuring these frequencies for various diameters of YIG spheres in an air dielectric stripline structure at 5 Gc.

The results of this investigation are shown in Fig. 8 which is a plot of the measured values of K^2 [calculated from (15)] vs the diameter of the spheres used. Using (14b) with the relevant parameter values ($r_0 = 0.15$ inch, $4\pi M = 1750$ gauss, $Z_{01} = 100\ \Omega$) the theoretical curve is also plotted in Fig. 8. Agreement is seen to be good except at the largest values of coupling where the observed coupling is reduced from the theoretical value. The disagreement is believed to be caused by the failure of dipolar fields to adequately describe the coupling when the sample diameter approaches the loop diameter.

Using the design procedure outlined in Section IV, a filter was designed using 0.003 inch copper stripline in irradiated polyethylene dielectric[6] with quarter wave sections of high impedance transmission line for the end sections. The impedance of the quarter wavelength lines was varied in order to vary the end coupling and hence the external $Q(Q_{1,3})$. The ferrimagnetic material was yttrium iron garnet with a line width of 0.5 oe which corresponds to an unloaded Q of 2800 at C-band. The sphere diameter was 0.105 inch. The response characteristics are shown in Fig. 9. With an external Q of 17.6 it is seen that the system has two well defined normal modes (the microwave circuit resonators had the same resonant frequency which reduces the number of normal modes from three to two) as discussed in [12]. The value of $K(K = 0.54)$ calculated from these two frequencies using (15) agrees closely with the value given in Fig. 8 (measured curve). For tighter coupling the loaded Q's of the normal modes are lowered resulting in the band-pass filter characteristic shown for $Q_e = 9.80$ and 3.52. In the latter case, the bandwidth was observed to be over 1 Gc. The observed bandwidth with $Q_e = 3.52$ (25 per cent) is smaller than predicted by the curve in Fig. 7 (45 per cent) since K is observed to be reduced from the theoretical result for large samples as shown in Fig. 8. For larger input microwave powers the response of the filter is limited as shown in Fig. 10 for the case $Q_e = 9.8$. The threshold power for limiting is in the milliwatt range in contrast with previously reported experiments using narrow bandwidth filters [9]. The theoretical limiting threshold calculated from (18) and Suhl's theory [8] for h_{crit} agrees in order of magnitude with the experimental values. The uncertainty in the theoretical result is partly due to uncertainties in the value of the spin wave linewidth for the particular spin waves excited in the first order instability. The limiting curves were taken with a fixed dc magnetic field. The dynamic limiting range of this limiter was typically 25 db. For frequencies outside of the band shown in Fig. 10 the dynamic range becomes significantly degraded. The bandwidth over which limiting is observed is indicated

[5] Dynamic range denotes the range of input power above the threshold over which the output power remains constant, say to within one db.

[6] Manufactured by Tellite Corp., Orange, N. J.

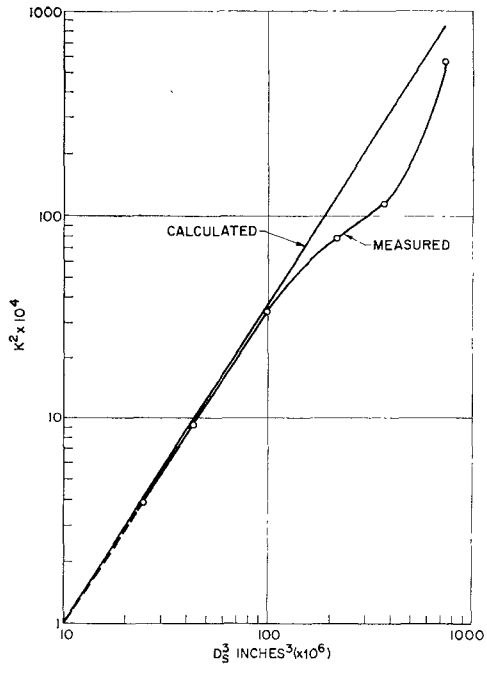

Fig. 8—Measured value of coupling coefficient vs diameter of yttrium iron garnet sphere. The calculated value corresponds to Z_{01} (resonator) = 100 Ω, r_0 = 0.150 inch.

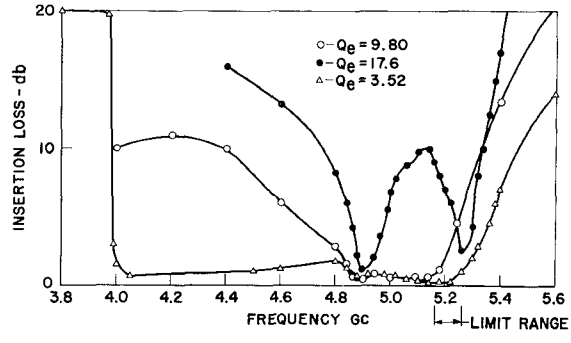

Fig. 9—(After Comstock and Dean [11]) Measured response of C-band ferrimagnetic filter for 3 values of filter end coupling. The yttrium iron garnet sphere diameter was 0.105 inch.

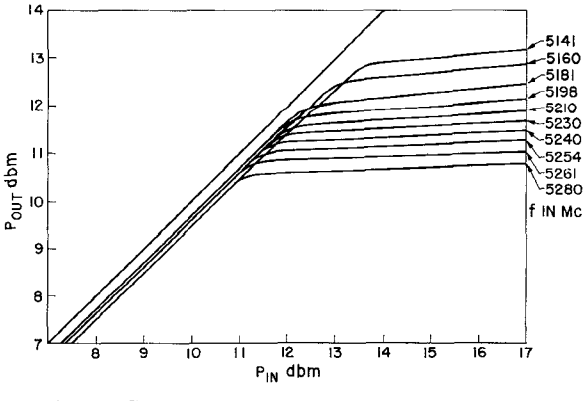

Fig. 10—(After Comstock and Dean [11]) Limiting characteristic taken with filter having characteristics given in Fig. 9. The external Q was 9.8. For frequencies outside the band shown the dynamic range is degraded.

on Fig. 9 which illustrates the conclusion made in [11] that first order process limiting for $\omega > (2/3)\omega_n$ should be observed only in the vicinity of the higher frequency normal mode.

In order to raise the threshold power level with a fixed bandwidth and dynamic range for this class of limiters, it has been found feasible to use ferrimagnetic materials with wider linewidths. As shown in [8] the threshold field is directly proportional to the ferromagnetic resonance linewidth for the first order process. For example, a limiter using terbium doped yttrium iron garnet [14] ($\Delta H \approx 2.3$ oe), has been constructed with the characterstics shown in Table I. The characteristics obtained with undoped YIG are also shown in this table. With a 0.5 db increase in insertion loss the threshold is seen to increase by 9 db using the wider linewidth material with a 3 db decrease in dynamic range. Another approach to increasing the threshold is to use samples with unpolished surfaces since then the contribution to the linewidth from surface scattering can dominate the loss mechanism [15]. Wide-band crossed stripline filter-limiters have also been made with polycrystal YIG ($\Delta H \approx 30$ oe) in which case the limiting thresholds are typically a watt or more.

TABLE I

Operating Characteristics of Strip-Line Filter-Limiter

	YIG (ΔH = 0.5 oe)	0.02 per cent Tb doped YIG (ΔH = 2.3 oe)
Operating Frequency	2.43 Gc	2.88 Gc
Bandwidth	90 Mc	60 Mc
Threshold (P_{crit})	−6 dbm	+ 3 dbm
Dynamic Range	25 db	22 db
Insertion Loss ($P < P_{crit}$)	0.5 db	1 db

Recently first order process power limiting was reported at X-band using lithium ferrite [12]. A photograph of the X-band filter-limiter is shown in Fig. 11. The stripline resonators are shown crossed over in the center of the ground plane (the top ground plane is removed). The high impedance lines are quarter wavelength coupling sections. The spherical sample is placed between the two resonators and biased with a dc magnetic field normal to the ground planes. The limiting characteristics are shown in Fig. 12. The filter bandwidth of this limiter was 320 Mc and limiting with a reasonably flat slope was observed over approximately 100 Mc. The dynamic range using low average power to avoid heating effects exceeded 25 db. The preliminary design of this limiter based on the results shown in Fig. 7 for a diameter of 0.024 inch predicted a bandwidth of approximately 10 per cent while the observed was closer to 4 per cent. However, the coupling constant was difficult to estimate since the coupling loops were far from circular in this case.

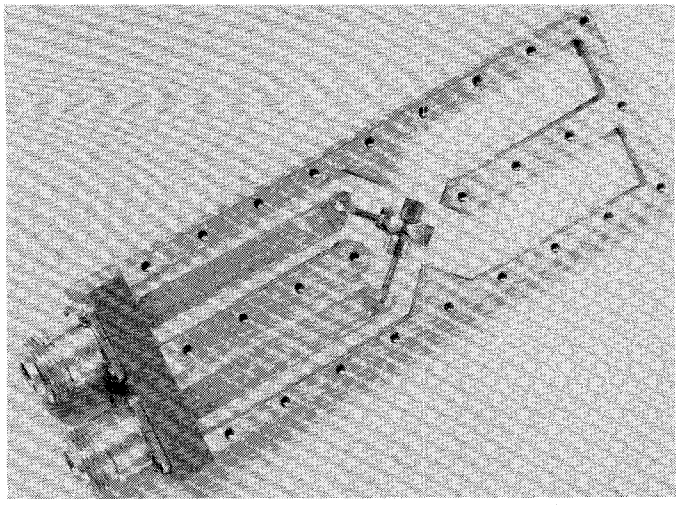

Fig. 11—Photograph of X-band crossed strip line filter-limiter. The lithium ferrite sample is placed between the two half-wave resonators (shown necked down in the center).

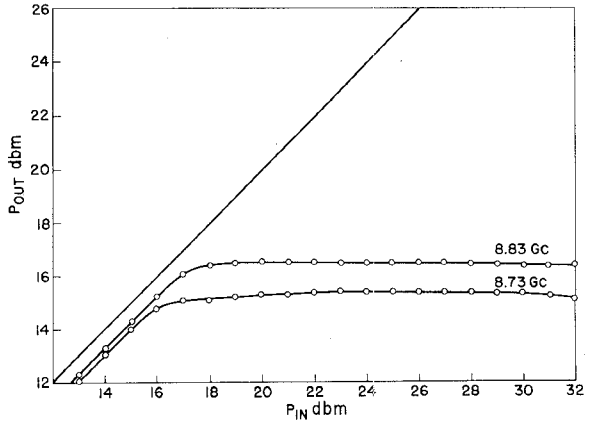

Fig. 12—(After Comstock and Loewy [12]) Limiting characteristics taken at X-band with lithium ferrite filter-limiter Fig. 11.

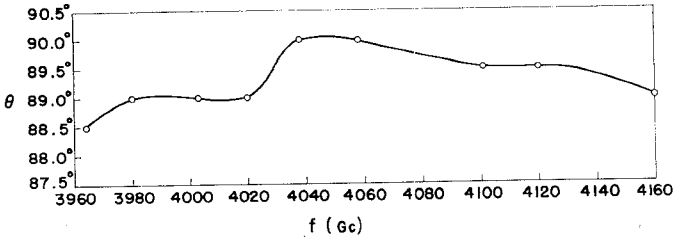

Fig. 13—Nonreciprocal phase characteristic of 4-Gc filter using YIG showing gyrator action.

The nonreciprocal phase shift of two of the stripline filters has been measured. For the lithium ferrite X-band filter the differential phase shift was measured with a microwave bridge which included a precision phase shifter and was found to be $\pm(90° \pm 2°)$ over a 170-Mc bandwidth [16]. Similar measurements were made on a 4-Gc ferrimagnetic filter using YIG and the results are shown in Fig. 13, which is a plot of one-half the measured differential phase shift vs frequency. The gyrator element formed from the ferrimagnetic filter has been found useful in constructing hybrid-gyrator four-port circulators [16].

VII. Conclusions

The theory of dipolar coupling presented in this paper has been found useful in preliminary design of ferrimagnetically coupled filter-limiters. The ferrimagnetic sample, when excited in the uniform precession mode, behaves in much the same way as a microwave cavity and can thus be incorporated into microwave filter structures. In particular, ferrimagnetic resonators have been found to be useful in conjunction with stripline circuitry in building wide- or narrow-band microwave filters. The first order spin wave instability has been found to result in excellent limiting characteristics in these filters. Limiting occurs over the entire filter bandwidth only if $\omega < (2/3)\omega_m$. For frequencies not satisfying this condition limiting occurs near the upper band edge of the filter response. By varying the linewidth of the uniform precession, by either varying the sample polish or by adding impurities such as the rare earths to narrow linewidth yttrium iron garnet, the limiting threshold can be changed with only a small variation in insertion loss. The nonreciprocal phase shift of these filters has been demonstrated and shown to be useful in constructing gyrators.

References

[1] R. W. De Grasse, "Low-loss gyromagnetic coupling through single crystal garnets," *J. Appl. Phys.*, Supp. to vol. 30, pp. 1558–1568; 1959.
[2] P. S. Carter, Jr., "Magnetically-tunable microwave filters using single-crystal yttrium iron garnet resonators," IRE Trans. on Microwave Theory and Techniques, vol. MTT-9, pp. 252–260; May, 9161.
[3] L. K. Anderson and H. J. Shaw, "The representation of waveguides containing small ferrimagnetic ellipsoids," presented at the PGMTT National Symposium, Boulder, Colo.; May, 1962.
[4] M. Dishal, "Design of dissipative band pass filters producing exact amplitude-frequency characteristics," Proc. IRE, vol. 37, pp. 1050–1069; September, 1949.
[5] J. J. Taub and B. F. Bogner, "Design of three-resonator dissipative band-pass filters having minimum insertion loss," Proc. IRE, vol. 45, pp. 681–687; May, 1957.
[6] S. B. Cohn, "Direct-coupled resonator filters, Proc. IRE, vol. 45, pp. 187–196, February, 1957; and "Dissipation loss in multiple-coupled resonator filters," Proc. IRE, vol. 47, pp. 1342–1348, August, 1959.
[7] G. L. Ragan, "Microwave Transmission Circuits," Radiation Laboratory Series, vol. 9, McGraw-Hill Book Co., Inc., New York, N. Y., 1948.
[8] H. Suhl, "The nonlinear behavior of ferrites at high signal levels," Proc. IRE, vol. 44, pp. 1270–1284; October, 1956.
[9] F. J. Sansalone and E. G. Spencer, "Low-level microwave power limiter," IRE Trans. on Microwave Theory and Techniques, vol. MTT-9, pp. 272–273; May, 1961.
[10] F. C. Rossol, "Power limiting in the 4-kMc to 7-kMc frequency range using lithium ferrite," Proc. IRE, vol. 49, p. 1574; October, 1961.
[11] R. L. Comstock and W. A. Dean, "Extension of coincidence limiting frequency range in ferrimagnets," *J. Appl. Phys.*, vol. 34, pp. 1275–1277; April, 1963.
[12] R. L. Comstock and M. Loewy, "An X-band coincidence ferrimagnetic limiter using lithium ferrite," Proc. IEEE (*Correspondence*), vol. 51, pp. 1769; December, 1963.
[13] J. Clark and J. Brown, "A miniaturized ferrimagnetic high power coaxial duplexer-limiter," *J. Appl. Phys.*, vol. 33, pp. 1270–1271S; March, 1962.
[14] J. F. Dillon, Jr. and J. W. Nielsen, "Effects of rare earth impurities on ferrimagnetic resonance in yttrium iron garnet," *Phys. Rev. Letters*, vol. 3, July, 1959.
[15] R. C. LeCraw, E. G. Spencer, and C. S. Porter, "Ferrimagnetic line width in yttrium iron garnet single crystals," *J. Appl. Phys.*, vol. 29, pp. 429–430; March, 1958.
[16] R. L. Comstock, "A cryogenic four-port circulator using single crystal yttrium iron garnet," Proc. IEEE (*Correspondence*), vol. 51, p. 1769; December, 1963.